Mon. Not. R. Astron. Soc. **288,** L39–L43 (1997)

Class II methanol maser candidates

A. M. Sobolev,[1⋆] D. M. Cragg[2⋆] and P. D. Godfrey[2⋆]
[1]*Astronomical Observatory, Ural State University, Lenin Street 51, Ekaterinburg 620083, Russia*
[2]*Department of Chemistry, Monash University, Clayton, Victoria 3168, Australia*

Accepted 1997 April 23. Received 1997 April 18; in original form 1997 March 19

ABSTRACT

Model spectra are presented for Class II methanol masers under a variety of conditions. The model is that of Sobolev & Deguchi, which includes pumping through levels of the second and first torsionally excited states. All the currently identified Class II methanol masers appear as strong masers in one or more of the model regimes, and a number of new maser candidates are identified.

Key words: masers – H II regions – ISM: molecules – radio lines: ISM.

1 INTRODUCTION

The strong methanol masers are associated with regions of active star formation. They fall into two categories according to their strongest maser transitions, denoted Class I and Class II (Batrla et al. 1987; Menten 1991). Class I sources are usually situated apart from compact continuum sources. In contrast, Class II methanol masers are usually found close to ultracompact H II regions.

Extensive surveys carried out recently (see e.g. Caswell et al. 1995; Ellingsen et al. 1996b) have shown that the Class II methanol maser phenomenon is very widespread. This result adds to the importance of understanding the nature of Class II methanol maser sources, which may be done through detailed studies of particular sources in various transitions.

Class II methanol masers include the extremely bright 6- and 12-GHz lines, as well as maser emission at 19 GHz (Wilson et al. 1985), 23 GHz (Wilson et al. 1984), 28 GHz (Wilson et al. 1993), 37 and 38 GHz (Haschick, Baan & Menten 1989), and 107 GHz (Val'tts et al. 1995), and a series at 157 GHz (Slysh, Kalenskii & Val'tts 1995).

The search for new methanol maser transitions is still in progress. Thus the publication of a list of candidate Class II methanol maser transitions, which provides guidelines for the search, is timely.

A number of publications contain a list of candidate Class II methanol maser transitions (e.g., Cragg et al. 1992; Sobolev 1993). However, the results of these papers are based either on models that do not reproduce the observed brightness of the strongest lines, or only on some general regularities found in detected masers.

A pumping mechanism operating through the levels of torsionally excited states, suggested in the paper of Sobolev & Deguchi (1994a, hereafter SD94) and further explored by Sobolev, Cragg & Godfrey (1997, hereafter SCG97), is able to explain the observed brightnesses of the 6- and 12-GHz maser lines as well as their ratio. Here we examine the other Class II methanol maser transitions predicted by this model.

⋆E-mail: Andrej.Sobolev@usu.ru (AMS); Dinah.Cragg@sci.monash.edu.au (DMC); Peter.Godfrey@sci.monash.edu.au (PDG)

This paper aims to reproduce spectra of Class II methanol masers over a wide frequency range. Since the parameter space of the model is enormous, for this initial investigation we have chosen several sets of parameters which correspond to some important regimes with differing spectra.

2 DESCRIPTION OF PRESENTED MODELS

In making the choice of models to present, we took into account the fact that extremely strong 6- and 12-GHz masers can arise over a wide range of physical parameters.

For example, in some sources bright maser spots are projected apart from the strong continuum source (Ellingsen, Norris & McCulloch 1996a) while all the maser spots in W3(OH) are seen in projection on the strong emission in the free–free continuum (Menten et al. 1988). To reflect these differences we have considered Class II methanol maser formation with two types of background continuum source: 2.7-K microwave background only, and a diluted free–free continuum source. The latter causes substantial saturation effects in the 6- and 12-GHz transitions when dilution is low (dilution factor $W_{\rm H\,II} = 2\times10^{-3}$ in our models). It should be noted that the case with a greatly diluted strong continuum source (when $W_{\rm H\,II} = 10^{-5}$, saturation does not play an important role in our models) can be reproduced by multiplying the brightness temperature of the line in the 2.7-K case by a factor of $T_{\rm bg}/(2.7\,{\rm K})$, where $T_{\rm bg}$ is the brightness temperature of the background source at the corresponding frequency. A similar approach can be used in order to take into account diluted emission of underlying dust, etc.

Hydrogen number density in strong Class II methanol masers can vary over a wide range. For example, in one of the strongest sources, NGC 6334F (6-GHz flux $F_6 = 3910$ Jy), the methanol masers are likely to be produced in a circumstellar disc (see, e.g., Ellingsen et al. 1996a) with considerable density. The other strongest Class II methanol maser source, W3(OH) ($F_6 = 3880$ Jy), shows different properties of the maser environment (see e.g. Wink et al. 1994). The results of SCG97 show that methanol masers in W3(OH) are likely to be produced in the low-density regime. We have chosen values of

$n_H = 10^4$ and 10^7 cm^{-3} because they well represent sources with low and high density, respectively.

The influence of the gas kinetic temperature has been explored by calculating models with $T_{kin} = 30$ and 150 K.

The great influence of beaming (expressed in large velocity gradient calculations by the ratio of the optical depths in the radial and tangential directions, ε^{-1}) on intensities of the strong Class II methanol masers was shown by SD94 and SCG97. Different possibilities in the beaming of the sources are modelled by values of $\varepsilon^{-1} = 1$ and 10.

For the temperature of the dust providing microwave photons for maser pumping, we have chosen the value $T_d = 175$ K [if $T_d < 150$ K, pumping does not operate efficiently, while $T_d = 200$ K is close to the highest dust temperatures observed in relevant sources: see e.g. Wink et al. (1994)].

The brightness temperature of the strong maser lines is mainly determined by the value of optical depth in the radial direction. In large velocity gradient modelling, its value is proportional to the product of the specific column density in the tangential direction, $N_M/\Delta V$ (where N_M is the methanol column density and ΔV is the line width), and the beaming factor ε^{-1}. With the same values of excitation temperature and background brightness, that term ultimately determines the strength of the maser line. In the models presented we chose $\varepsilon^{-1}N_M/\Delta V = 10^{12.5}$ cm^{-3} s, in order to reproduce the high observed brightness temperature of the 6-GHz line in the models with $T_{kin} = 30$ K.

Energy levels up to $J = 20$ for torsional state $v_t = 0$, 1, 2 were calculated from the Hamiltonian of Mekhtiev & Godfrey (1996).

3 DESCRIPTION OF THE SPECTRA

In Fig. 1 we present model spectra with frequencies below 200 GHz. In each plot two spectra are superimposed, to illustrate the difference between two model regimes. The transitions, as well as higher frequency lines, are identified in Table 1.

It is immediately apparent that no other masers attain the extreme brightness temperatures found in the 6- and 12-GHz lines ($> 10^{10}$ K). There are, however, approximately 100 other transitions which display Class II maser character under appropriate model conditions with predicted brightness temperature $> 10^4$ K. All of the 18 transitions that have been identified in the literature as observed Class II methanol masers are present in our list of strong masers. Of these, 17 transitions attain brightness temperatures $> 10^6$ K in one or more regimes of our calculations (the remaining line, $1_0 - 1_{-1}$E, being relatively weak both in observations and in modelling, is subject to overlap effects which will be considered in a future publication). There are a considerable number of new transitions which attain a similar level of brightness (Table 1), and thus represent the best candidates for new methanol maser identifications. Unfortunately the best of these fall in the frequency range 50–70 GHz, which makes them unsuitable for terrestrial observation. There are fewer bright lines above 200 GHz.

It is also clear from Fig. 1 that the relative brightness of the masers depends sensitively on the model parameters (note the log scale). It is hoped that this information will eventually be used to define the physical conditions in individual maser spots when masers at several frequencies are known to be coincident. For example, the 37-GHz $7_{-2} - 8_{-1}$ E maser appears only in high-density calculations, whereas the 38-GHz $6_2 - 5_3$ A species doublet becomes a strong maser only at low density.

The masers are generally brighter in the high-density, low-temperature regime, with beamed geometry and a greatly diluted

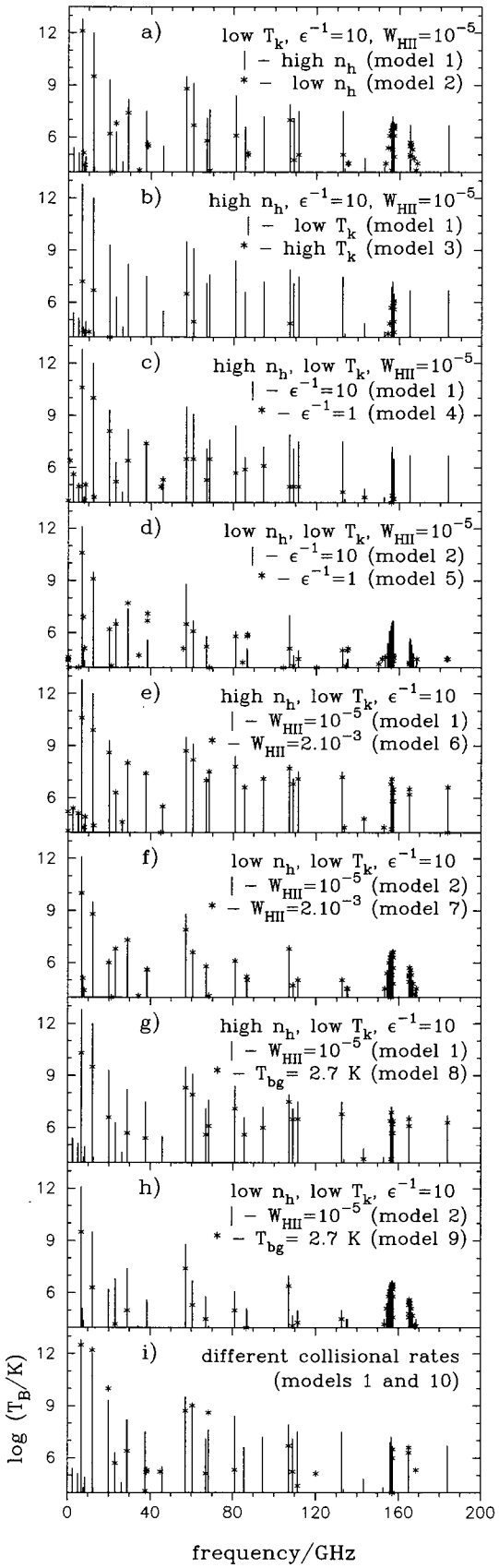

Figure 1. Comparison of spectra in different model regimes.

Table 1. Brightness temperatures for the models displayed in various combinations in Fig. 1. Models 8 and 9 have no underlying H II region continuum, and model 10 has non-selective collisional excitation rates. All transitions with brightness temperatures > $10^{4.5}$ K in one or more models are tabulated. Brightness temperatures > 10^6 K are shown bold for emphasis. All transitions with brightness temperatures > 10^4 K are inverted. Transitions that have been identified observationally as Class II masers are marked *. Frequencies are from laboratory measurements by the following authors: A = Anderson, De Lucia & Herbst (1990); AC = calculated by A; B = Breckenridge & Kukolich (1995); R = Radford (1972); T = Tsunekawa et al. (1995); or are calculated according to D = De Lucia et al. (1989).

			MODEL		1	2	3	4	5	6	7	8	9	10	
			T_{kin}		30	30	150	30	30	30	30	30	30	30	
			$\log(n_H)$		7	4	7	7	4	7	4	7	4	7	
			ε^{-1}		10	10	10	1	1	10	10	10	10	10	
			$\log(W_{H\,II})$		−5	−5	−5	−5	−5	−2.7	−2.7			−5	
			T_d		175	175	175	175	175	175	175	175	175	175	
			$\log(N_M/\Delta V)$		11.5	11.5	11.5	12.5	12.5	11.5	11.5	11.5	11.5	11.5	
v_t	TRANSITION		FREQ/MHz		LOG(BRIGHTNESS TEMPERATURE/K)										ref
0	2(2)A+	2(2)A−	2.271		5.2	< 3	< 3	3.9	< 3	5.2	< 3	< 3	< 3	< 3	D
0	3(2)A+	3(2)A−	11.354		< 3	3.7	< 3	< 3	4.5	< 3	3.9	< 3	< 3	< 3	D
0	6(2)A+	6(2)A−	158.841		3.8	< 3	< 3	3.5	4.6	3.9	< 3	< 3	< 3	3.1	D
0	1(1)A−	1(1)A+	834.267		< 3	< 3	< 3	**6.4**	3.0	< 3	< 3	< 3	< 3	< 3	R
0	2(1)A−	2(1)A+	2502.778		5.4	< 3	< 3	5.6	< 3	5.4	< 3	< 3	< 3	< 3	A
0	3(1)A−	3(1)A+	5005.321		5.1	< 3	< 3	4.9	4.0	5.1	3.3	< 3	< 3	< 3	B
0	5(1)A+	6(0)A+	6668.519	*	**12.8**	**12.1**	**7.2**	**10.6**	**10.6**	**10.6**	**10.0**	**10.3**	**9.5**	**12.5**	B
0	11(−3)E	10(−4)E	7283.110		< 3	5.1	4.4	< 3	**6.9**	< 3	5.1	< 3	< 3	< 3	AC
0	12(4)A−	13(3)A−	7682.232		4.3	4.4	< 3	4.1	5.1	4.3	4.4	< 3	< 3	< 3	T
0	12(4)A+	13(3)A+	7830.864		4.3	4.4	< 3	4.1	5.1	4.3	4.4	< 3	< 3	< 3	T
0	4(1)A−	4(1)A+	8341.622		4.9	3.0	< 3	5.0	3.8	4.9	3.3	< 3	< 3	3.9	B
0	2(0)E	3(−1)E	12178.597	*	**12.0**	**9.5**	**6.7**	**10.0**	**9.1**	**9.9**	**8.8**	**9.5**	**6.3**	**12.2**	B
0	2(1)E	3(0)E	19967.390	*	**9.3**	**6.2**	4.0	**8.1**	**6.2**	**8.6**	**6.0**	**6.6**	3.5	**10.0**	T
0	9(2)A+	10(1)A+	23121.024	*	**6.3**	**6.8**	3.4	5.2	**6.5**	**6.3**	**6.8**	3.6	4.2	5.7	T
0	11(2)E	11(1)E	26313.113		4.6	< 3	< 3	< 3	< 3	4.6	< 3	< 3	< 3	< 3	T
0	8(2)A−	9(1)A−	28969.942	*	**8.2**	**7.4**	3.3	**6.4**	**7.7**	**8.0**	**7.3**	5.7	5.0	**6.4**	T
0	14(−3)E	15(−2)E	34236.943		3.5	4.1	< 3	3.5	4.7	3.5	4.1	< 3	< 3	< 3	T
0	7(−2)E	8(−1)E	37703.700	*	**7.5**	< 3	< 3	**7.4**	< 3	**7.4**	< 3	5.4	< 3	4.1	T
0	6(2)A−	5(3)A−	38293.268	*	< 3	5.6	3.9	< 3	**6.7**	< 3	5.6	< 3	3.5	5.2	T
0	6(2)A+	5(3)A+	38452.677	*	< 3	5.5	3.9	< 3	**7.1**	< 3	5.6	< 3	3.4	5.3	T
1	2(0)E	3(1)E	44955.807		4.0	< 3	< 3	4.9	3.3	4.0	< 3	< 3	< 3	5.2	T
0	9(3)E	10(2)E	45843.519		5.5	3.4	< 3	5.3	3.8	5.5	3.4	3.5	< 3	< 3	T
0	12(−3)E	11(−4)E	55673.867		< 3	3.2	3.6	< 3	5.1	< 3	3.2	< 3	< 3	< 3	T
0	4(1)A+	5(0)A+	57032.941		**9.5**	**8.8**	**6.5**	**6.5**	**6.5**	**8.7**	**7.9**	**8.3**	**7.4**	**8.7**	T
0	1(0)E	2(−1)E	60531.469		**9.1**	**6.7**	**4.9**	**6.5**	**6.1**	**8.2**	**6.6**	**7.9**	**5.3**	**9.0**	T
0	8(2)A+	9(1)A+	66947.909		**7.1**	5.8	< 3	5.3	5.2	**7.0**	5.8	5.6	4.5	5.1	T
0	1(1)E	2(0)E	68305.645		**7.6**	**4.1**	< 3	**6.5**	**4.0**	**7.5**	**4.1**	**6.1**	< 3	**8.6**	T
0	7(2)A−	8(1)A−	80993.230		**8.4**	**6.1**	< 3	5.7	5.8	**7.8**	**6.1**	**7.1**	5.0	5.3	T
0	6(−2)E	7(−1)E	85568.084		**6.6**	< 3	< 3	5.9	< 3	**6.6**	< 3	5,6	< 3	< 3	T
0	7(2)A−	6(3)A−	86615.578		< 3	5.1	3.5	< 3	5.8	< 3	5.2	< 3	4.0	3.4	T
0	7(2)A+	6(3)A+	86902.956		< 3	5.0	3.5	< 3	5.9	< 3	5.0	< 3	3.9	3.3	T
0	8(3)E	9(2)E	94541.778		**7.2**	< 3	< 3	**6.1**	< 3	**7.1**	< 3	**6.0**	< 3	< 3	T
0	3(1)A+	4(0)A+	107013.812	*	**7.9**	**7.0**	4.8	4.9	5.1	**7.7**	**6.8**	**7.5**	**6.4**	**6.7**	T
0	0(0)E	1(−1)E	108893.948		**7.1**	4.7	3.4	4.9	4.1	**6.8**	4.7	**6.5**	4.1	5.2	T
0	7(2)A+	8(1)A+	111289.515		**7.5**	5.0	< 3	4.9	4.5	**7.1**	5.0	**6.5**	4.3	4.4	T
0	3(1)E	2(2)E	120197.532		< 3	3.7	< 3	< 3	4.0	< 3	3.7	< 3	< 3	5.1	T
0	6(2)A−	7(1)A−	132621.787		**7.5**	5.0	< 3	4.6	5.0	**7.2**	5.0	**6.8**	4.5	3.9	T
0	8(2)A−	7(3)A−	134896.881		< 3	4.5	3.3	< 3	5.0	< 3	4.5	< 3	3.9	< 3	T
0	8(2)A+	7(3)A+	135376.853		< 3	4.5	3.3	< 3	5.1	< 3	4.5	< 3	3.9	< 3	T
0	7(3)E	8(2)E	143169.532		4.8	< 3	< 3	4.3	< 3	4.8	< 3	4.2	< 3	< 3	T
0	13(0)E	13(−1)E	151860.198		< 3	3.6	3.2	< 3	4.5	< 3	3.6	< 3	3.4	< 3	T
0	12(0)E	12(−1)E	153281.604		< 3	4.5	3.7	< 3	4.6	< 3	4.5	< 3	4.2	< 3	T
0	11(0)E	11(−1)E	154425.806		3.2	5.4	4.2	3.0	4.6	3.3	5.4	3.0	5.1	< 3	T
0	10(0)E	10(−1)E	155320.795		3.4	**6.1**	4.8	< 3	4.7	3.4	**6.0**	3.3	5.8	< 3	T
0	9(0)E	9(−1)E	155997.463		< 3	**6.4**	5.7	< 3	4.7	< 3	**6.3**	< 3	**6.1**	< 3	T
0	6(2)A+	7(1)A+	156127.673		**6.9**	4.1	< 3	4.0	4.1	**6.8**	4.0	**6.4**	3.8	3.2	T
0	8(0)E	8(−1)E	156488.868	*	4.3	**6.6**	5.7	< 3	4.7	4.2	**6.5**	4.2	**6.3**	< 3	T
0	2(1)A+	3(0)A+	156602.413	*	**7.2**	5.3	3.7	4.4	4.2	**7.1**	5.3	**6.9**	5.0	3.0	T
0	7(0)E	7(−1)E	156828.533	*	5.9	**6.7**	5.8	3.5	4.7	5.8	**6.6**	5.7	**6.4**	< 3	T

Table 1 – *continued*

v_t	TRANSITION		FREQ/MHz		LOG(BRIGHTNESS TEMPERATURE/K)										ref
			MODEL		1	2	3	4	5	6	7	8	9	10	
0	6(0)E	6(−1)E	157048.625	*	**6.3**	**6.7**	**6.0**	4.2	4.7	**6.3**	**6.6**	**6.2**	**6.5**	4.0	T
0	5(0)E	5(−1)E	157179.017	*	5.8	**6.7**	**6.1**	3.9	4.7	5.8	**6.6**	5.7	**6.5**	**6.0**	T
0	4(0)E	4(−1)E	157246.056	*	**6.5**	**6.6**	5.6	4.2	4.7	**6.5**	**6.6**	**6.4**	**6.4**	**6.5**	T
0	1(0)E	1(−1)E	157270.851	*	< 3	4.9	3.7	< 3	3.9	< 3	4.8	< 3	4.6	< 3	T
0	3(0)E	3(−1)E	157272.369	*	< 3	**6.5**	4.9	< 3	4.6	< 3	**6.3**	3.2	**6.2**	< 3	T
0	2(0)E	2(−1)E	157276.058	*	< 3	**6.1**	4.3	< 3	4.4	< 3	5.7	< 3	5.8	< 3	T
0	1(1)E	1(0)E	165050.195		**6.7**	4.9	< 3	< 3	4.3	**6.5**	4.9	**6.5**	4.6	**6.6**	T
0	2(1)E	2(0)E	165061.156		**6.3**	5.0	< 3	< 3	4.2	**6.2**	5.2	**6.1**	4.8	**6.3**	T
0	3(1)E	3(0)E	165099.271		< 3	5.5	< 3	< 3	4.3	< 3	5.3	< 3	5.3	< 3	T
0	4(1)E	4(0)E	165190.498		< 3	5.7	< 3	< 3	4.2	< 3	5.7	< 3	5.5	< 3	T
0	5(1)E	5(0)E	165369.371		< 3	5.7	< 3	< 3	3.9	< 3	5.7	< 3	5.6	< 3	T
0	6(1)E	6(0)E	165678.670		< 3	5.6	< 3	< 3	3.8	< 3	5.6	3.0	5.4	< 3	T
0	7(1)E	7(0)E	166169.143		< 3	5.3	< 3	< 3	3.7	< 3	5.3	< 3	5.1	< 3	T
0	8(1)E	8(0)E	166898.615		< 3	4.8	< 3	< 3	3.7	< 3	4.8	< 3	4.7	< 3	T
0	4(1)E	3(2)E	168577.860		< 3	4.5	< 3	< 3	4.5	< 3	4.5	< 3	4.1	5.3	T
0	9(2)A−	8(3)A−	183123.833		< 3	3.9	3.1	< 3	4.5	< 3	3.9	< 3	3.6	< 3	T
0	5(2)A−	6(1)A−	183852.770		**6.7**	3.8	< 3	3.3	3.8	**6.6**	3.6	**6.3**	3.6	< 3	T
0	9(2)A+	8(3)A+	183879.928		< 3	3.9	3.1	< 3	4.5	< 3	3.9	< 3	3.6	< 3	T
0	5(2)A+	6(1)A+	201445.590		5.7	3.5	< 3	< 3	3.6	5.7	3.4	5.5	3.4	< 3	A
0	1(1)A+	2(0)A+	205791.270		**6.0**	3.2	< 3	3.9	3.0	**6.0**	3.2	5.9	3.1	< 3	A
0	5(1)E	4(2)E	216945.600		< 3	5.0	< 3	< 3	4.3	< 3	5.0	< 3	4.7	3.2	A
0	4(2)A−	5(1)A−	234683.390		5.2	3.2	< 3	< 3	3.2	5.2	3.1	5.1	3.1	< 3	A
0	4(2)A+	5(1)A+	247228.693		**6.3**	3.3	< 3	< 3	3.6	**6.3**	3.4	**6.1**	3.2	< 3	A
1	5(1)A+	6(2)A+	263793.856		3.3	< 3	< 3	3.6	< 3	3.3	< 3	3.1	< 3	4.9	A
1	5(1)A−	6(2)A−	265224.400		3.3	< 3	< 3	3.7	< 3	3.3	< 3	3.1	< 3	5.0	A
0	6(1)E	5(2)E	265289.650		< 3	4.9	< 3	< 3	4.1	< 3	4.9	< 3	4.8	< 3	A
0	9(−3)E	10(−2)E	281956.350		4.7	3.4	< 3	3.9	3.6	4.7	3.4	4.6	3.3	< 3	AC
0	3(2)A−	4(1)A−	285111.150		4.7	< 3	< 3	< 3	< 3	4.7	< 3	4.7	< 3	< 3	A
0	3(2)A+	4(1)A+	293463.990		5.8	< 3	< 3	< 3	3.2	5.8	< 3	5.7	< 3	< 3	A
1	4(1)A+	5(2)A+	312247.354		3.5	< 3	< 3	3.5	< 3	3.5	< 3	3.4	< 3	5.4	A
1	4(1)A−	5(2)A−	313203.428		3.4	< 3	< 3	3.6	< 3	3.4	< 3	3.3	< 3	5.5	A
0	7(1)E	6(2)E	313596.840		< 3	4.6	< 3	< 3	3.9	< 3	4.6	< 3	4.5	< 3	A
0	9(1)A−	9(0)A+	322239.450		4.7	4.0	3.0	3.3	3.9	4.8	4.1	4.7	4.0	< 3	A
0	10(1)A−	10(0)A+	326630.610		4.8	3.9	3.0	3.4	3.8	4.8	3.9	4.7	3.9	< 3	A
0	8(−3)E	9(−2)E	330793.909		4.9	3.3	< 3	3.7	3.4	4.8	3.3	4.7	3.2	< 3	A
1	3(1)A+	4(2)A+	360661.433		3.7	< 3	< 3	3.6	< 3	3.7	< 3	3.6	< 3	5.6	A
1	3(1)A−	4(2)A−	361236.476		3.6	< 3	< 3	3.7	< 3	3.6	< 3	3.5	< 3	5.7	A
0	7(−3)E	8(−2)E	379493.994		5.0	3.1	< 3	3.6	3.3	5.0	3.1	4.9	3.1	< 3	A
1	2(1)A+	3(2)A+	409035.534		3.7	< 3	< 3	3.5	< 3	3.7	< 3	3.6	< 3	5.6	A
1	2(1)A−	3(2)A−	409323.292		3.5	< 3	< 3	3.5	< 3	3.5	< 3	3.4	< 3	5.6	A
0	6(−3)E	7(−2)E	428087.588		4.7	< 3	< 3	3.5	3.1	4.8	< 3	4.7	< 3	< 3	A
1	1(1)A+	2(2)A+	457367.889		3.8	< 3	< 3	3.5	< 3	3.8	< 3	3.7	< 3	5.6	A
1	1(1)A−	2(2)A−	457463.899		3.7	< 3	< 3	3.5	< 3	3.7	< 3	3.7	< 3	5.5	A
1	4(−2)E	5(−3)E	633584.860		3.5	< 3	< 3	3.1	< 3	3.5	< 3	3.5	< 3	4.8	D
1	3(−2)E	4(−3)E	681802.566		3.8	< 3	< 3	3.2	< 3	3.8	< 3	3.8	< 3	5.1	D
1	2(−2)E	3(−3)E	730026.534		4.0	< 3	< 3	3.2	< 3	4.0	< 3	3.9	< 3	5.1	D

background H II region continuum source. At low density the masers generally become weaker (Fig. 1a), although there are some lines that become stronger, in addition to the 38-GHz doublet discussed above. These changes are attributed to the effects of collisions, which become significant in the pumping at high densities. At even higher densities the masers are quenched altogether (see e.g. the results of SCG97).

Fig. 1(b) shows the effects of kinetic temperature in the high-density regime. At low temperature many masers are present, but these are progressively quenched as the kinetic temperature is raised. In contrast, at low density the pattern of excitation is independent of the kinetic temperature, and the brightness of masers remains at the same level even when the kinetic temperature exceeds the dust temperature. In this case the pumping mechanism is ultimately controlled by radiative processes.

Figs 1(c) and (d) show the effect of beamed geometry. It is clearly seen that the strongest masers are brighter in the beamed case. This comes about from the fact that (with the same value of $\varepsilon^{-1}N_M/\Delta V$) the integrated escape probability in the thermal pumping lines is higher in the beamed case. Hence radiative–radiative pumping is more efficient. However, the situation is actually more complicated, especially for the weaker masers. In methanol we have the case of 'interacting maser transitions' when plenty of pump cycle links correspond to maser transitions (see Sobolev & Deguchi 1994b).

This results in a lower brightness of some maser transitions when beaming is included. The effect is more pronounced in the low-density regime when collisions do not interfere in the pumping (Fig. 1d).

In Figs 1(e) and (f) we compare models with different values of the H II region dilution factor. The brightest masers appear when the free–free continuum background is extremely diluted. When the continuum source is brought closer to the maser region, the effects of saturation are evident in the brightest lines. More of the unsaturated lines are affected at high densities because of the collisional coupling.

In Figs 1(g) and (h), models with and without the background H II region continuum source are compared. Amplification of the background continuum results in brighter masers, particularly at lower frequencies where the H II region emission is stronger. This effect is more evident at low densities, without the interference of collisional coupling.

The calculations reported here were done with the collisional excitation model of Peng & Whiteoak (1993). Calculations with a non-selective collision model generated spectra of somewhat different appearance in the high-density regime (Fig. 1i), but were unchanged at low density. An improved collision model is required for the reliable modelling of methanol masers under high-density conditions.

4 DISCUSSION AND CONCLUSION

This paper presents a variety of possible spectra of Class II methanol maser sources in a number of important cases. All observed Class II methanol maser transitions become masers in our model. Since the transitions exhibit different sensitivity to variation in the model parameters, future modelling of particular maser spots should allow the nature of their sources to be distinguished. For example, the difference between the two brightest 6-GHz sources is noticable in the weaker maser lines, NGC 6334F being much stronger then W3(OH) in the weaker lines while their 6-GHz fluxes are similar.

A few transitions from Table 1 are worthy of special mention. A number of the previously identified Class II masers have only been reported in a few sources, and further observations or upper limits would provide valuable constraints for modelling (e.g. the 28-GHz $8_2 - 9_1\,A^-$ line). The low-frequency A species K doublet transitions, such as the 834-MHz $1_1 - 1_1$ A line, are especially sensitive to small changes in the collision rates, suggesting that the model predictions are unreliable in this case. Detection of methanol masers in torsionally excited states would be a valuable test of the pumping model, and Table 1 includes a few such weak maser candidates. Of these, the 45-GHz $2_0 - 3_1\,v_t = 1$ E line is the most promising. The best new promising maser candidates are in the 50–70 GHz range, but the following lines are also good prospects: $7_2 - 8_1\,A^-$ at 80 GHz and A^+ at 111 GHz, $8_3 - 9_2$ E at 94 GHz, $0_0 - 1_{-1}$ E at 108 GHz, and $6_2 - 7_1\,A^-$ at 132 GHz, and the 165-GHz $J_1 - J_0$ E series.

ACKNOWLEDGMENTS

The authors thank Dr M. A. Mekhtiev for providing energy levels and line strengths for methanol. DMC and PDG thank the Australian Research Council for financial support. AMS thanks the Russian Foundation for Fundamental Research for financial support (grant 96-02-19689), and is grateful to the University of Sydney Research Centre for Theoretical Astrophysics for the opportunity to visit Australia and complete this work.

REFERENCES

Anderson T., De Lucia F. C., Herbst E., 1990, ApJS, 72, 797
Batrla W., Matthews H. E., Menten K. M., Walmsley C. M., 1987, Nat, 326, 49
Breckenridge S. M., Kukolich S. G., 1995, ApJ, 438, 504
Caswell J. L., Vaile R. A., Ellingsen S. P., Whiteoak J. B., Norris R. P., 1995, MNRAS, 272, 96
Cragg D. M., Johns K. P., Godfrey P. D., Brown R. D., 1992, MNRAS, 259, 203
De Lucia F. C., Herbst E., Anderson T., Helminger P., 1989, J. Molec. Spectrosc., 134, 395
Ellingsen S. P., Norris R. P., McCulloch P. M., 1996a, MNRAS, 279, 101
Ellingsen S. P., von Bibra M. L., McCulloch P. M., Norris R. P., Deshpande A. A., Phillips C. J., 1996b, MNRAS, 280, 378
Haschick A. D., Baan W. A., Menten K. M., 1989, ApJ, 346, 330
Mekhtiev M. A., Godfrey P. D., 1996, J. Mol. Spectrosc., 180, 54
Menten K. M., 1991, ApJ, 380, L75
Menten K. M., Reid M. J., Moran J. M., Wilson T. L., Johnston K. J., Batrla W., 1988, ApJ, 333, L83
Peng R. S., Whiteoak J. B., 1993, MNRAS, 260, 529
Radford H. E., 1972, ApJ, 174, 207
Slysh V. I., Kalenskii S. V., Val'tts I. E., 1995, ApJ, 442, 668
Sobolev A. M., 1993, Sov. Astron. Lett., 19, 293
Sobolev A. M., Deguchi S., 1994a, A&A, 291, 569 (SD94)
Sobolev A. M., Deguchi S., 1994b, ApJ, 433, 719
Sobolev A. M., Cragg D. M., Godfrey P. D., 1997, A&A, in press (SCG97)
Tsunekawa S., Ukai T., Toyama A., Takagi K., 1995, report for the Grant-in-aid for Scientific Research on Priority Areas (Interstellar Matter, 1991–1994) of the Ministry of Education, Science, and Culture, Japan. Toyama University, Japan
Val'tts I. E., Dzura A. M., Kalenskii S. V., Slysh V. I., Booth R. S., Winnberg A., 1995, A&A, 294, 825
Wilson T. L., Walmsley C. M., Snyder L. E., Jewell P. R., 1984, A&A, 134, L7
Wilson T. L., Walmsley C. M., Menten K. M., Hermsen W., 1985, A&A, 147, L19
Wilson T. L., Hüttemeister S., Dahmen G., Henkel C., 1993, A&A, 268, 249
Wink J. E., Duvert G., Guilloteau S., Güsten R., Walmsley C. M., Wilson T. L., 1994, A&A, 281, 505

This paper has been typeset from a TEX/LATEX file prepared by the author.